Infrared absorptions of $NH_3(H_2)$ complexes trapped in solid neon

Marilyn E. Jacox[a] and Warren E. Thompson[b]
Optical Technology Division, National Institute of Standards and Technology, Gaithersburg, Maryland 20899-8441

(Received 29 November 2005; accepted 10 March 2006; published online 22 May 2006)

When a very small concentration of H_2 is added to a $Ne:NH_3=800:1$ sample and the resulting mixture is deposited at 4.3 K, a new absorption appears at 4151.1 cm^{-1} which can be assigned to the H_2 stretching fundamental of H_2 $(j=1)$ complexed with NH_3. Other new absorptions which appear near the vibrational fundamentals of NH_3 are assigned to the NH_3 moiety in this complex and in the complex of NH_3 with H_2 $(j=0)$. The results of experiments in which HD or D_2 is added to the $Ne:NH_3$ mixture support these assignments. *Ab initio* and density functional calculations predict the observed infrared activation of the H_2-stretching vibration for a structure in which the axis of the H_2 molecule is collinear with the threefold axis of the NH_3. The dependence of the observed absorption patterns on the concentration of H_2 in the sample indicates that complexes of NH_3 with two or more H_2 molecules also form readily. [DOI: 10.1063/1.2192519]

I. INTRODUCTION

Little is known about the formation of complexes between NH_3 and H_2. As part of a search for NH_5, Olah *et al.*[1] conducted CNDO/2 calculations for the linear $HH-NH_3$ species, which they found to be a weakly bonded complex. Later, *ab initio* studies[2–4] were conducted on inelastic collisions between the various nuclear spin isomers of NH_3 and H_2 and on the rates of rotational energy transfer between these two species at low temperatures. These studies have contributed to our understanding of the results of microwave double resonance, pressure broadening, and crossed-beam measurements on mixtures of NH_3 and H_2, as well as to the elucidation of astrophysical phenomena.[4,5] Spectroscopic observations of the $NH_3(H_2)$ system may contribute to the development of a molecular basis for the hydrogen storage capability of ammonia and its derivatives.

Studies of the isoelectronic $H_2\cdots HF$ complex provide useful information regarding the expected properties of $NH_3(H_2)$. *Ab initio* calculations for the $H_2\cdots HF$ complex[6] found a global minimum for a T-shaped structure, bound by approximately 3.6 kJ/mol (300 cm^{-1}), with the H atom of the HF closest to the H_2 molecule. The lowest energy linear structure, $HF\cdots HH$, was a saddle point on the potential surface. In high-resolution gas-phase studies of the infrared spectrum of the HF-stretching fundamental of the complex, Lovejoy *et al.*[7] and Jucks and Miller[8] identified only transitions of the Π state of the T-shaped complex with H_2 $(j=1)$. Lovejoy *et al.*[9] later saw bands arising from both $j=0$ and $j=1$ levels of D_2 in its complex with HF. Although the Π complex is approximately 20 cm^{-1} more strongly bound than the Σ complex, both have similar structures. The only spectroscopic information regarding the H_2 moiety in the $H_2\cdots HF$ complex was obtained in neon-matrix observations by Hunt and Andrews,[10] who identified the H_2-stretching absorption at 4155 cm^{-1}.

Another isoelectronic complex, $H_2O\cdots H_2$, has often been studied. Early experimental investigations of the complexation of H_2 by amorphous ice spurred a series of *ab initio* calculations,[11,12] which established the existence of a primary potential minimum with a depth of approximately 2.4 kJ/mol, with H_2O the proton acceptor. The H_2 is complexed at the O atom, with the H–H axis collinear with the H_2O symmetry axis. For the secondary minimum, with a depth of approximately 2.2 kJ/mol, H_2O serves as the proton donor. The structure is analogous to that found for $H_2\cdots HF$, and the $H_2\cdots H$ plane is perpendicular to that of the H_2O moiety. Diffusion Monte Carlo calculations[12] indicate that H_2 $(j=0)$ forms a complex with a H atom of H_2O, whereas H_2 $(j=1)$ can form a complex either at one of the H atoms or at the O atom of H_2O. Weida and Nesbitt[13] analyzed three bands in the H_2O ν_2 spectral region. All of them arose from the axial complex of H_2 $(j=1)$, but both nuclear spin modifications of the H_2O moiety were represented. Recently, Fajardo *et al.*[14] observed the complexation of H_2O and of D_2O with the residual H_2 $(j=1)$ in a *p*-H_2 matrix. Another study, by Forney *et al.*,[15] reported that even for very dilute $Ne:H_2:H_2O$ deposits the dipole-forbidden vibrational fundamental absorption of H_2 appears, together with new peaks contributed by the H_2O moiety in the complex. The failure to detect new absorptions for $Ne:HD:H_2O$ deposits suggests that complexation occurs preferentially with H_2 $(j=1)$.

Very recently, Fawzy *et al.*[16] reported a fluorescence excitation spectrum for the $A\,^3\Pi-X\,^3\Sigma^-$ transition of the $H_2\cdots NH$ complex. Their calculations predicted a binding energy of approximately 1.4 kJ/mol (116 cm^{-1}), as well as a secondary minimum for a T-shaped structure analogous to that of $H_2\cdots HF$. They suggested that the primary minimum is contributed by the complex with H_2 $(j=1)$ and the secondary minimum by that with H_2 $(j=0)$.

In an argon-matrix study by Moroz *et al.*[17] of the infra-

[a]Electronic mail: marilyn.jacox@nist.gov
[b]Guest researcher at the National Institute of Standards and Technology.

red and Raman spectra of van der Waals complexes between H_2 and various Lewis bases, including NH_3, the dipole-forbidden infrared absorption of the vibrational fundamental of H_2 was detected. For NH_3, this absorption appeared 5 cm^{-1} below the absorption assigned to the H_2 moiety of $H_2O\cdots H_2$. Only a single broad absorption appeared in the NH_3 ν_2 spectral region, and its maximum shifted as a function of the H_2 concentration, typically several mole percent.

Recently, we reported the stabilization of NH_4^+ and its isotopomers in solid neon, using several different discharge sampling configurations for ion production.[18] Typical samples contained five or six times as much H_2 (or D_2) as NH_3, contained in a large excess of neon. Both the H_2 and the NH_3 concentrations were much lower than those used by Moroz *et al.* Under the conditions of our experiments, the ν_2 absorption of NH_3 was highly structured. However, this structure was very different from that for NH_3 in the absence of H_2, for which assignments of the various peaks to transitions involving rotation and inversion of the NH_3 have been proposed.[19,20] In the following discussion, the results of spectroscopic observations on $Ne:NH_3=800:1$ deposits to which various concentrations of H_2, HD, or D_2 had been added will be reported and analyzed.

II. EXPERIMENTAL DETAILS[21]

The NH_3 sample used for these studies (Matheson Gas Products, Inc.) was freed of relatively volatile impurities by freezing at 77 K and pumping on the solid sample. The H_2 and D_2 (Matheson Gas Products, Inc.), HD (97%, Cambridge Isotope Laboratories, Inc.), and neon (Spectra Gases, Inc., Research Grade, 99.999%) were used without further purification. Samples were prepared using standard vacuum procedures. All of the samples had the mole ratio $Ne:NH_3:H_2\text{-}d_n=800:1:x$, where $x=0$, 0.25, 0.50, 1, or (for H_2) 6. They were deposited and maintained at approximately 4.3 K in a Helitran (APD Cryogenics, Inc.) continuous transfer liquid helium cell. In order to facilitate comparisons in product yield, amounts of sample which varied by less than 5% were deposited in the experiments for which $x=0.25$, 0.50, or 1.

The absorption spectra of the sample deposits were obtained using a Bomem DA 3.002 Fourier transform interferometer with transfer optics that have been described previously.[22] Observations were conducted with a resolution of 0.2 cm^{-1} between 450 and 5000 cm^{-1} using a globar source, a KBr beamsplitter, and a wide-band HgCdTe detector cooled to 77 K. Data were accumulated for each spectrum over a period of at least 15 min. The resulting spectrum was ratioed against a similar one taken without a deposit on the cryogenic mirror. Under these conditions, the positions of the prominent, nonblended atmospheric water vapor lines between 1385 and 1900 cm^{-1} and between 3620 and 3900 cm^{-1}, observed in a calibration scan, agreed to within 0.01 cm^{-1} with the high-resolution values reported by Toth.[23] Based on previous investigations, with this experimental configuration the standard uncertainty (type B) in the determination of the positions of absorption maxima for molecules trapped in solid neon is ± 0.1 cm^{-1} (coverage factor, $k=1$, i.e., 1σ).

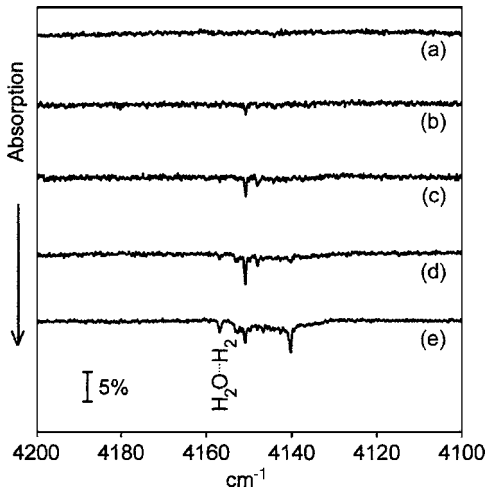

FIG. 1. Spectral region of H_2 vibrational fundamental observed for $Ne:NH_3:H_2=800:1:x$ deposits. (a) 6.50 mmol $Ne:NH_3=800:1$ deposited at 4.3 K over a period of 66 min. (b) 6.53 mmol $Ne:NH_3:H_2=800:1:0.25$ deposited at 4.3 K over a period of 73 min. (c) 6.62 mmol $Ne:NH_3:H_2=800:1:0.50$ deposited at 4.3 K over a period of 72 min. (d) 6.57 mmol $Ne:NH_3:H_2=800:1:1$ deposited at 4.3 K over a period of 68 min. (e) 6.87 mmol $Ne:NH_3:H_2=800:1:6$ deposited at 4.3 K over a period of 73 min.

III. RESULTS AND DISCUSSION

A. Infrared activation of H_2 and D_2

As is shown in Fig. 1(b), even for a deposit which has a mole ratio $Ne:NH_3:H_2=800:1:0.25$ a weak new absorption is discernible at 4151.1 cm^{-1}. This peak is shifted farther from the gas-phase band centers for H_2 [$Q_1(0)=4161.134$ cm^{-1}, $Q_1(1)=4155.201$ cm^{-1}] (Ref. 24) than the 4156.9 cm^{-1} peak assigned to the $H_2O\cdots H_2$ complex,[15] suggesting that NH_3 forms a complex with H_2 that is slightly more strongly bound than $H_2O\cdots H_2$. As the concentration of H_2 is increased [cf. Figs. 1(c)–1(e)], satellite peaks appear and grow. The first of these to appear are a peak at 4148.2 cm^{-1} and two partially resolved peaks at 4152.8 and 4153.4 cm^{-1}. As is shown in Fig. 1(b) of the earlier study of the spectrum of the $H_2O\cdots H_2$ complex,[15] for 9.37 mmol of a simple $Ne:H_2=800:1$ deposit the only absorption in this spectral region was an approximately 2% absorbing peak at 4156.9 cm^{-1}, contributed by $H_2O\cdots H_2$. That complex was formed because of the desorption of traces of H_2O from the walls of the vacuum system. Therefore, none of the peaks in the present experiments which have $Ne:H_2$ mole ratios equal to or greater than 800:1 could have been contributed by $(H_2)_n$ aggregates. When the concentration of H_2 exceeds that of NH_3, as in the experiment of Fig. 1(e), the prominent peak at 4151.1 cm^{-1} and the peak at 4148.2 cm^{-1} diminish in intensity, and a new peak at 4140.3 cm^{-1} grows. The increasing complexity of the observed absorption pattern as the H_2 concentration increases suggests that reactions of additional H_2 molecules with the initially formed species occur readily.

For the $Ne:NH_3:HD=800:1:1$ deposit, the only new

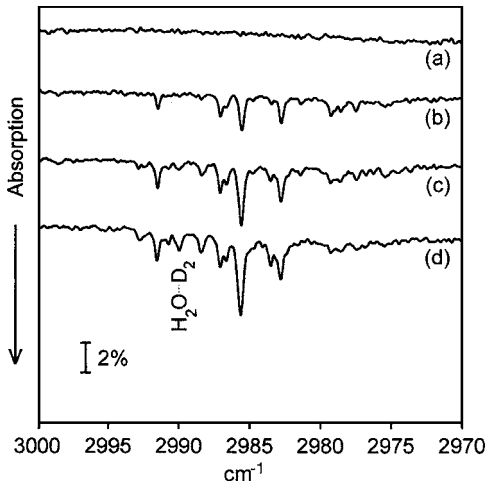

FIG. 2. Spectral region of D_2 vibrational fundamental observed for $Ne:NH_3:D_2=800:1:x$ deposits. (a) 16.20 mmol $Ne:NH_3=800:1$ deposited at 4.3 K over a period of 164 min. (b) 19.38 mmol $Ne:NH_3:D_2=800:1:0.25$ deposited at 4.3 K over a period of 218 min. (c) 19.38 mmol $Ne:NH_3:D_2=800:1:0.50$ deposited at 4.3 K over a period of 217 min. (d) 20.20 mmol $Ne:NH_3:D_2=800:1:1$ deposited at 4.3 K over a period of 210 min.

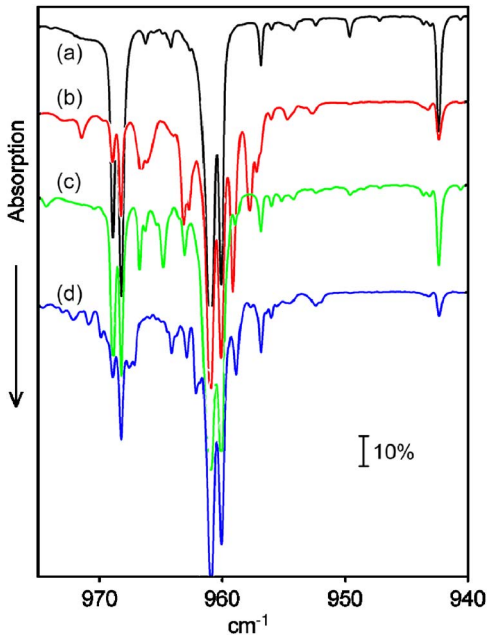

FIG. 3. (Color online) Dependence of absorption pattern in the spectral region of NH_3 ν_2 on isotopic composition of H_2 in $Ne:NH_3:H_2$-$d_n=800:1:1$ deposits, compared to the spectrum observed in the absence of H_2. (a) 6.50 mmol $Ne:NH_3=800:1$ deposited at 4.3 K over a period of 66 min. (b) 6.57 mmol $Ne:NH_3:H_2=800:1:1$ deposited at 4.3 K over a period of 68 min. (c) 6.46 mmol $Ne:NH_3:HD=800:1:1$ deposited at 4.3 K over a period of 68 min. (d) 6.46 mmol $Ne:NH_3:D_2=800:1:1$ deposited at 4.3 K over a period of 68 min.

peaks detected near the gas-phase HD band center $[Q_1(0)=3632.055\ cm^{-1}]$ (Ref. 24) are a weak absorption at 3630.6 cm^{-1} and very weak absorptions at 3614.7, 3615.8, and 3634.7 cm^{-1}.

As is shown in Fig. 2(b), even for the $Ne:NH_3:D_2=800:1:0.25$ deposit several new absorptions appear near the gas-phase D_2 band centers $[Q_1(0)=2993.548\ cm^{-1}$, $Q_1(1)=2991.446\ cm^{-1}]$.[24] The most prominent of these lies at 2985.7 cm^{-1}, but somewhat less intense absorptions are evident at 2982.9, 2987.1, and 2991.6 cm^{-1}, as well as somewhat weaker absorptions between 2977.6 and 2979.3 cm^{-1}. These absorptions become stronger, the spectrum becomes somewhat more complex, and the 2990.9 cm^{-1} peak previously assigned[15] to $H_2O\cdots D_2$ appears at higher concentrations of D_2, illustrated by Figs. 2(c) and 2(d).

B. Behavior of absorptions associated with NH_3 vibrations

All of the other new absorptions which appear on adding H_2, HD, or D_2 to the sample mixtures lie close to absorptions of NH_3. However, their positions vary somewhat, depending on the isotopomer of H_2 which is added to the sample. These variations are especially marked in the NH_3 ν_2 spectral region, illustrated in Fig. 3 for $Ne:NH_3:H_2$-$d_n=800:1:1$ deposits. The spectrum shown in Fig. 3(a) was taken for a simple $Ne:NH_3=800$ deposit. As is shown in Fig. 3(b), when H_2 is present in the sample several new absorptions appear. The most prominent of these are at 957.7, 959.1, 963.1, and 966.6 cm^{-1}. The positions and approximate relative intensities of all of the new peaks observed in the NH_3 absorption regions for a $Ne:NH_3:H_2=800:1:1$ deposit are summarized in the first column of Table I. In the experiment of Fig. 3(b), not only did these new absorptions appear but also the NH_3 absorptions common to Fig. 3(a) decreased in intensity. This decrease is most noticeable for the NH_3 absorptions at 942.4, 968.2, and 968.9 cm^{-1}, previously assigned[20] to the site II *a* $Q(1,1)$, site I *a* $R(0,0)$, and site I *s* $Q(1,1)$ transitions of NH_3, respectively.

When HD was instead added to the sample, the spectrum shown in Fig. 3(c) resulted. Several new absorptions appear, including those at 959.0, 963.1, 964.8, and 966.7 cm^{-1}. A complete summary of the new peaks which appear in the regions of NH_3 absorptions is given in the second column of Table I. The prominent new peak at 964.8 cm^{-1} does not correspond to an absorption in the experiments in which H_2 is present. As is shown in Fig. 3(c), the intensities of the NH_3 absorptions are somewhat decreased from those of the $Ne:NH_3$ deposit.

Figure 3(d) shows the spectrum obtained when D_2 was added to the sample. New absorptions appeared at 958.9 and 962.9 cm^{-1}, as did shoulders on the 968.2 cm^{-1} NH_3 peak, at 967.1 and 967.6 cm^{-1}. These and other new absorptions are summarized in the third column of Table I. The decrease in the peak optical densities of the NH_3 absorptions, evident in Fig. 3(d) for the peaks at 942.4, 968.2, and 968.9 cm^{-1}, is similar to or somewhat greater than that for samples to which H_2 has been added.

New absorptions which appear in the higher frequency NH_3 absorption regions when H_2, HD, or D_2 is added to the sample are included in Table I. In the ν_4 spectral region, new peaks appear in the H_2-containing samples at 1617.9, 1634.0, and 1635.0 cm^{-1}. In the presence of HD, a shoulder appears at 1637.2 cm^{-1} and a new peak at 1638.2 cm^{-1}. For samples doped with D_2, there are new peaks at 1618.1, 1633.7, 1634.9, and 1637.4 cm^{-1}. All of the NH_3 absorptions de-

TABLE I. Absorptions (cm^{-1}) which appear in regions of the NH_3 fundamentals and overtones for $Ne:NH_3:H_2-d_n=800:1:1$ deposits but not for a $Ne:NH_3=800:1$ deposit, with tentative rotational assignments for the H_2-d_n moiety. [*w*—weak, *m*—medium, *s*—strong, sh—shoulder, and br—broad. Peaks which are especially prominent in the spectrum of a $Ne:NH_3:H_2=800:1:6$ sample are designated by (*M*). Based on previous investigations, the standard uncertainty (type B) in the frequency measurement is ±0.1 cm^{-1} (coverage factor, $k=1$; i.e., 1σ).]

H_2	HD	D_2	Assignment
954.7 *wm*			
957.2 sh			
957.7 *m*			$j=1$
959.1 *s*	959.0 *wm*	958.9 *m*	$j=0$
962.7 sh		962.1 sh	
963.1 *s* (*M*)	963.1 *m*	962.9 *m*	$j=0$
		963.7 sh	
	964.8 *ms*		$j=0$
966.6 *m* (*M*)	966.7 *ms*		$j=0$
		967.1 sh	
		967.6 sh	
969.6 *vw* (*M*)			
		969.9 *wm*	
		970.8 *wm*, br	
971.4 *m* (*M*)			
		972.1 *wm*, br	
	974.3 *wm*, br		
1617.9 *wm*		1618.1 *m*	$j=1$
		1633.7 *wm*	
1634.0 *m* (*M*)			
1635.0 *m*		1634.9 *m*	$j=1$
	1637.2 *wm*, sh	1637.4 *wm*	$j=0$
	1638.2 *wm*		$j=0$
		3241.6 *w*	
3249.7 *w*, br	3249.7 *wm*	3250.0 *wm*	$j=0$
3318.4 *w*	3319.1 *wm*	3318.8 *wm*	$j=0$
3332.9 *wm*		3332.9 *wm*	$j=1$
3443.5 *w*, br (*M*)			
3447.5 sh	3448.6 *w*, sh	3446.9 *wm*	$j=0$

crease, but especially large changes are noted for the peaks at 1610.5 and 1644.8 cm^{-1} when H_2 or D_2 is present in the sample.

For samples containing H_2, HD, and D_2, a new, rather broad peak appears at or near 3249.7 cm^{-1}, only 2 cm^{-1} above the peak previously assigned[20] to the perpendicular component of NH_3 $2\nu_4$ $a\,{}^rR(0,0)$. The latter peak is appreciably decreased in intensity when H_2 or D_2 is present in the deposit.

In the ν_1 spectral region, when either H_2 or D_2 is present in the deposit a sharp new absorption appears at 3332.9 cm^{-1}. In these same deposits, the ν_1 $a\,R(0,0)$ absorption of NH_3, at 3350.2 cm^{-1}, is markedly diminished in intensity.

A relatively broad shoulder appears on the low frequency side of the NH_3 ν_3 $a\,{}^rR(0,0)$ peak at 3453.0 cm^{-1}. When H_2 is present, the maximum of this absorption lies at 3447.5 cm^{-1}, and when D_2 is present, at 3446.9 cm^{-1}. In both of these systems, the intensity of the 3453.0 cm^{-1} absorption is considerably reduced from that for the $Ne:NH_3=800:1$ deposit. When HD is present, a weak new absorption appears at 3448.6 cm^{-1}, and the intensity of the 3453.0 cm^{-1} absorption is similar to that in the absence of HD.

As already illustrated, addition of H_2 to the $Ne:NH_3$ sample results in a larger decrease in the peak optical densities of the absorptions of NH_3 in its $j=1$, $k=1$ states than in those of NH_3 in its $j=0$, $k=0$ state. The calculation[3,4] of a larger cross section for inelastic collisions of H_2 ($j=1$) with NH_3 than for inelastic collisions of H_2 ($j=0$) with NH_3 is consistent with this observation.

Complex formation between H_2 and NH_3 trapped in site I also appears to be favored. The extent of this selectivity is underestimated in the observed spectrum, as some complexation occurs in the gas-phase sample mixture and in the deposition system. As was suggested by Abouaf-Marguin *et al.*[19] and supported by the recent studies of the infrared spectra of $Ne:NH_3$ deposits,[20] it is likely that NH_3 trapped in site II has the relatively ordered environment provided by a double substitutional site in the solid neon lattice, whereas NH_3 trapped in site I has a less ordered environment, with greater crowding by adjacent atoms and molecules. In this less ordered environment, there would be a greater probability for one or more H_2 molecules to be a nearest neighbor to an NH_3 molecule, favoring complex formation.

Although much less NH_3 participates in complex formation when HD is present than when H_2 or D_2 is present in the sample, the intensities of all of the NH_3 absorptions are consistently reduced by the introduction of HD into the sample mixture.

The data summarized in Table I facilitate the tentative assignments of the j value of the H_2-d_n moiety given in the fourth column. At 4.3 K, almost all of the HD is thermally deactivated to its $j=0$ state. However, because of their very slow rate of nuclear spin conversion H_2 and D_2 each have appreciable populations of the nuclear spin isomer for which $j=1$ (*ortho*-H_2, *para*-D_2). The observations are consistent with the hypothesis that all three H_2 isotopomers in their $j=0$ states can form complexes with NH_3, but that the long-lived nuclear spin isomers of H_2 and D_2 with $j=1$ more readily complex with NH_3. Nuclear spin conversion of the NH_3 also occurs, but on the time scale of the experiments.[25] In this and the following discussion, isomerization of the relatively short-lived nuclear spin species of NH_3 will not be considered. In order to permit tentative assignments, it will be assumed that different sets of absorption frequencies of the NH_3 moiety result from complexation of H_2 ($j=0$) and of H_2 ($j=1$) and that on substitution of HD or of D_2 in the binary complex, any given frequency of the NH_3 moiety experiences a shift of only a few tenths of a wave number. The following two generalizations then lead to the assignments summarized in Table I:

(1) The $j=0$ complex should be observed in the presence of H_2, HD, and D_2.
(2) The $j=1$ complex should be observed for H_2 and D_2, but not for HD. However, because of the different nuclear spin degeneracies characteristic of H_2 and D_2, the concentration of D_2 ($j=1$) should be considerably smaller than that of D_2 ($j=0$).

Since in the Ne:NH_3:HD experiments the absorption in the HD spectral region is very weak compared to product absorptions in the NH_3 ν_2 spectral region, it is inferred that the absorptions arising from complexed H_2 and D_2 ($j=0$) are also relatively weak and that the HH-stretching absorption at 4151.1 cm^{-1} and the DD-stretching absorption at 2985.7 cm^{-1} are contributed by $NH_3(H_2)$ ($j=1$) and $NH_3(D_2)$ ($j=1$), respectively.

C. Concentration dependence of the absorption patterns

The spectra shown in Figs. 1 and 2 indicate that the absorption pattern resulting from complex formation between NH_3 and H_2-d_n is dependent on the concentration of hydrogen in the sample. The following consideration of the absorption patterns observed near the vibrational fundamentals of NH_3 supports this conclusion.

The positions and approximate relative intensities of all of the absorptions of NH_3-containing species observed for a Ne:NH_3=800:1 deposit and for Ne:NH_3=800:1 deposits to which various small concentrations of H_2 have been added are summarized in Table II. The assignments given in Table II for the transitions of uncomplexed NH_3 have previously been discussed.[20] Certain peaks of the complex appear to have a nonlinear dependence on the concentration of H_2. These are labeled in the assignment column by M, indicating that they are contributed by $NH_3(H_2)_n$ species for which $n>1$. The proposed assignments for the j value of the H_2 moiety of the binary complex (cf. Table I) are also included in Table II.

The spectra obtained in the 940–1040 cm^{-1} spectral region for samples containing various concentrations of H_2 are shown in Fig. 4. For all but Fig. 4(e), the spectra between 940 and 975 cm^{-1} are shown at an expanded scale in Fig. 5. [Figure 5(d) is the same as Fig. 3(b).] The decrease in several of the NH_3 peaks as the concentration of H_2 is increased is evident. Although most of the new absorptions appear to have an approximately linear dependence on the H_2 concentration, the peaks at 963.1 and 969.6 cm^{-1} increase very rapidly—but at different rates—at the higher H_2 concentrations. The peak at 971.4 cm^{-1} also has a nonlinear concentration dependence, but does not grow as rapidly as do the other two peaks. Because they grow irreversibly on slight warming of the deposit, several broad absorptions between 989 and 1050 cm^{-1} have long been attributed[19,26] to NH_3 trapped in a neon matrix. Analogs of these peaks in argon-matrix experiments have been studied by several workers,[19,26,27] and analyses of the spectrum of $(NH_3)_2$ between about 975 and 1010 cm^{-1} have been reported for the dimer in the gas phase[28] and in helium clusters.[29] Therefore, it is suggested that the addition of H_2 to the sample somewhat reduces the extent of isolation of NH_3 in neon. Although for a Ne:NH_3=800:1 mole ratio the random probability of nearest-neighbor pairs of NH_3 molecules in the neon matrix is extremely small, some dimer formation can occur in the gas-phase sample and on the surface of the deposit. The sticking probability for atoms and molecules colliding with the cryogenic surface is less than unity. This probability is especially small for H_2, which has an appreciable vapor pressure at 4.3 K. If a molecule collides with a surface molecule and there is a stable potential minimum for the dimer or multimer which would be formed, the sticking probability of the colliding molecule is enhanced. Furthermore, the role of defects, including larger vacancies, becomes increasingly important with higher concentrations of H_2 in the deposit. These defects may also promote the stabilization of larger clusters. Nevertheless, the spectra indicate that at Ne:H_2 mole ratios equal to or greater than 800:1 [as in all of the spectra except that of Fig. 4(e)] most of the NH_3 is well isolated. Some of the structure near 1000 cm^{-1} which appears at the higher concentrations of H_2 can also be attributed to the formation of $(NH_3)_x(H_2)_y$ aggregates. These new, incompletely resolved peaks are not included in Table II. The absorption at 1031.7 cm^{-1} is contributed by the $NH_3(H_2O)$ complex.[30]

As is shown in Fig. 6, as the concentration of H_2 is increased the complicated absorption pattern between 1635.5 and 1644.8 cm^{-1}, assigned to the ν_4 $a\,{}^rR(0,0)$ transition of NH_3 trapped in various sites in the neon matrix, steadily diminishes and is replaced by a new absorption at 1635.0 cm^{-1}. At higher H_2 concentrations another new absorption at 1634.0 cm^{-1} predominates, and can be attributed to species containing more than one H_2 molecule. A less prominent product absorption at 1617.9 cm^{-1} has an approximately linear dependence on the H_2 concentration. Although Süzer and Andrews[26] did not report any absorptions near 1618 cm^{-1} for relatively concentrated Ne:NH_3 deposits, Fig. 6(a) shows a very weak absorption at 1618.2 cm^{-1}, and an absorption in Ar:NH_3 deposits at 1618 cm^{-1} has been assigned[19] to an aggregate species. Therefore, an aggregate of NH_3 might contribute to the 1617.9 cm^{-1} absorption.

Figure 7 shows the H_2 concentration dependence of the absorption pattern in the region of the first overtone of ν_4 and of the NH-stretching fundamentals of NH_3. The new peak at 3249.7 cm^{-1} is relatively constant in intensity at the lower H_2 concentrations, but broadens to higher frequencies at higher H_2 concentrations. Süzer and Andrews[26] assigned a peak at 3253.3 cm^{-1} to $(NH_3)_2$ isolated in a neon matrix. They also assigned rather broad absorptions between 3314 and 3320 cm^{-1} and the peak near 3413 cm^{-1} to NH_3 aggregates, consistent with the assignments in the present study. In the present experiments, these broad absorptions change somewhat in frequency as the H_2 concentration is increased, suggesting that $(NH_3)_x(H_2)_y$ species may also contribute to the absorption. In the absence of H_2, very weak, sharp peaks appear at 3332.7 and 3334.2 cm^{-1}. On addition of H_2, a new, sharp peak appears at 3332.9 cm^{-1} and grows with increasing H_2 concentration, consistent with its contribution by the binary complex. The peak at 3334.2 cm^{-1} does not experience a similar growth. A shoulder at 3447.5 cm^{-1} probably is contributed by the ν_3 absorption of the binary complex of NH_3 with H_2. At higher H_2 concentrations, it is replaced by a broad absorption maximum at 3443.5 cm^{-1}.

Similar experiments were conducted on the dependence of the NH_3 absorption pattern on the concentration of HD or

TABLE II. Positions (cm^{-1}) and approximate relative intensities of absorptions which are observed for $Ne:NH_3=800:1$ deposits to which various concentrations of H_2 have been added. [*w*—weak, *m*—medium, *s*—strong, sh—shoulder, and br—broad. Peaks which are especially prominent in the spectrum of a $Ne:NH_3:H_2=800:1:6$ sample are designated by (*M*). Based on previous investigations, the standard uncertainty (type B) in the frequency measurement is ± 0.1 cm^{-1} (coverage factor, $k=1$; i.e., 1σ).]

$Ne:NH_3=800:1$	$Ne:NH_3:H_2=$ 800:1:0.25	$Ne:NH_3:H_2=$ 800:1:0.5	$Ne:NH_3:H_2=$ 800:1:1	$Ne:NH_3:H_2=$ 800:1:6	Assignment[a]	
940.6 *w*						
942.4 *ms*	942.4 *ms*	942.4 *m*	942.4 *m*	942.4 *vw*	NH_3 *a* $Q(1,1)$	II
949.6 *m*	949.6 *wm*	949.6 *w*	949.6 *vw*		NH_3 *a* $Q(1,1)$	I
954.2 *wm*	954.2 *wm*	954.2 *wm*	954.2 sh			
	954.7 sh	954.7 sh	954.7 *wm*	954.7 *w*, br		
956.8 *m*	956.8 *wm*	956.8 sh	956.8 sh	956.8 sh	NH_3 *s* $P(1,0)$	I
	957.2 sh	957.2 sh	957.2 sh	957.2 sh		
	957.8 *wm*	957.7 *m*	957.7 *m*	957.7 *m*	$j=1$	
	959.2 *m*	959.2 *ms*	959.1 *s*	959.1 *ms*	$j=0$	
960.1 *s*	960.1 *s*	960.1 *s*	960.1 *s*	960.1 *m*, br		
961.0 *vs*	960.9 *vs*	960.9 *vs*	960.9 *vs*	960.9 *s*	NH_3 *a* $R(0,0)$	II
	962.7 *w*, sh	962.7 *wm*, sh	962.7 sh	962.7 sh		
	963.1 *vw*	963.1 *wm*, br	963.1 *m*	963.1 *s*	$j=0$, *M*	
964.2 *wm*	964.2 *wm*	964.2 *wm*	964.2 *w*	964.2 *w*	NH_3 *s* $Q(1,1)$	II
966.2 *m*	966.2 *m*	966.2 *m*	966.1 sh	966.1 sh	NH_3 *a* $R(0,0)$	I
	966.6 *w*	966.6 *wm*	966.6 *m*	966.6 *s*	*M*	
968.2 *vs*	968.2 *vs*	968.2 *s*	968.2 *m*		NH_3 *a* $R(0,0)$	I
968.9 *s*	968.9 *s*	968.9 *ms*	968.9 *m*		NH_3 *s* $Q(1,1)$	I
			969.6 vw	969.6 *ms*	*M*	
		971.4 *vw*	971.4 *m*	971.4 *m*	*M*	
976.7 *wm*	976.7 *wm*	976.8 *w*	976.8 *w*	976.8 *w*	NH_3 *a* $R(1,1)$	II
981.5 *wm*, br	981.5 *m*, br	981.5 *m*, br	981.5 *m*, br	981.5 *wm*, br	$(NH_3)_n$	
993.2 *wm*	993.3 *m*	993.3 *m*	993.3 *m*		$(NH_3)_n$	
994.4 sh	994.4 sh	994.4 *m*	994.4 sh	994.4 sh	$(NH_3)_n$	
			995.2 *m*	995.2 *m*, br	$(NH_3)_n$	
			997.1 *m*	997.1 sh	$(NH_3)_n$	
998.5 *wm*					$(NH_3)_n$	
1019.4 *wm*, br	1019.4 *m*, br	1019.4 *m*, br	1019.2 *wm*, br	1019.2 *w*, br	$(NH_3)_n$	
1031.7 *m*	1031.7 *m*	1031.7 *m*	1031.7 *wm*	1031.7 *wm*	$NH_3(H_2O)$	
	1033.0 *w*	1033.0 *wm*	1033.0 *w*	1033.0 sh		
1600.5 *w*, br					NH_3 ν_4 *s*, *a* $^pP(1,1)$	I
1610.6 *wm*	1610.5 *wm*	1610.5 *wm*	1610.5 *w*	1610.5 *vw*, br	NH_3 ν_4 *s*, *a* $^pP(1,1)$	II
	1617.9 *w*	1617.9 *wm*	1617.9 *wm*	1617.9 sh	$j=1$	
				1618.7 *wm*	*M*	
				1619.3 *wm*	*M*	
				1619.9 sh	*M*	
1622.5 *w*						
				1623.3 *w*		
1624.8 *vw*					NH_3 ν_4 *s*, *a* $^pQ(1,1)$	II
1625.8 *vw*					NH_3 ν_4 *s*, *a* $^pQ(1,1)$	II
				1632.8 sh		
		1634.0 *wm*	1634.0 *m*	1634.0 *s*	*M*	
	1635.0 *wm*	1635.0 *m*	1635.0 *m*	1634.9 *ms*	$j=1$	
1635.5 *m*	1635.5 *m*	1635.5 *m*	1635.5 sh		NH_3 ν_4 *a* $^rR(0,0)$	I
1636.6 *s*	1636.7 *s*	1636.7 *s*	1636.7 *m*	1636.7 *w*	NH_3 ν_4 *a* $^rR(0,0)$	I
1640.1 *w*						
1640.9 *w*						
1642.3 *s*	1642.3 *s*	1642.3 *s*	1642.3 *m*	1642.3 *w*	NH_3 ν_4 *a* $^rR(0,0)$	II
1643.2 *vs*	1643.2 *vs*	1643.2 *vs*	1643.2 *ms*	1643.2 *wm*	NH_3 ν_4 *a* $^rR(0,0)$	II
1644.8 *s*	1644.8 *ms*	1644.8 *m*	1644.8 *wm*		NH_3 ν_4 *a* $^rR(0,0)$	II
3247.8 *wm*	3247.7 *wm*	3247.7 *wm*	3247.7 *w*		NH_3 $2\nu_4(\perp)$ *a* $^rR(0,0)$	
	3249.7 *vw*	3249.7 *vw*	3249.7 *w*, br	3250.7 *w*, br	$j=0$	
3253.6 *w*	3253.4 *w*				NH_3 $2\nu_4(\perp)$ *s*, *a* $^rR(1,1)$	
			3318.4 *w*	3318.4 *wm*	$j=0$	
	3319.8 *w*	3319.8 *w*				
	3332.9 *vw*	3332.9 *w*	3332.9 *wm*	3332.9 *wm*	$j=1$	
3350.2 *m*	3350.3 *m*	3350.3 *m*	3350.3 *wm*	3350.3 *vw*	NH_3 ν_1 *a* $R(0,0)$	II

TABLE II. (*Continued.*)

Ne:NH_3=800:1	Ne:NH_3:H_2= 800:1:0.25	Ne:NH_3:H_2= 800:1:0.5	Ne:NH_3:H_2= 800:1:1	Ne:NH_3:H_2= 800:1:6	Assignment[a]	
3364.8 *w*	3364.7 *w*	3364.7 *w*			NH_3 ν_1 *a R*(0,0)	I
				3407.6 *wm*, br		
			3409.7 *wm*, br			
	3412.4 *wm*, br	3412.3 *wm*, br				
3413.0 *w*, br						
				3431.1 *w*, sh		
			3443.5 *w*, br	3443.5 *wm*	*M*	
		3447.5 *w*, sh	3447.5 sh		*j*=0	
3453.0 *m*	3453.0 *m*	3453.0 *m*	3452.6 *w*		NH_3 ν_3 *a* ^{r}*R*(0,0)	II
3455.9 sh	3455.9 *m*	3455.9 *m*	3455.6 *vw*		NH_3 ν_3 *a* ^{r}*R*(0,0)	I
3466.2 *wm*					NH_3 ν_3 *a*,*s* ^{r}*R*(1,1)	
			4140.5 *vw*	4140.5 *wm*	*M*	
		4148.3 *vw*	4148.3 *vw*			
	4151.1 *vw*	4151.1 *w*	4151.1 *wm*	4151.1 *w*	*j*=1	
				4152.3 *vw*	*M*	
				4153.3 *vw*	*M*	
			4157.0 *vw*	4157.0 *w*	*M*	

[a]For uncomplexed NH_3, see Ref. 20 (I, II designate type of site in which the NH_3 is trapped.) For the binary complex, the tentative *j* value of the H_2 moiety is given. Absorptions contributed by ternary or larger clusters are designated by *M*.

of D_2 in the sample. The results of these experiments, summarized in Tables E-1 and E-2 and illustrated in Figs. E-1 and E-6 of the supplementary EPAPS file,[31] are consistent with those for the introduction of H_2 into the system.

D. Properties of binary complexes of NH_3 with H_2

As already noted, these experiments suggest that two distinct species occur for the binary complex of H_2 with NH_3, depending on whether the nuclear spin isomer of H_2 for which $j=0$ or that for which $j=1$ participates in the complex.

In order to obtain further information regarding the structures and energetics of these complexes, *ab initio* calculations were conducted for binary complexes of NH_3 with H_2 using the GAUSSIAN 03 program package.[32] These calculations were performed at the RMP2/6-311++G(3*df*,3*pd*) level, using the basis set superposition error (BSSE) correction.[33] Single-point calculations including the BSSE correction were also performed using the coupled cluster singles and doubles with perturbative triples [CCSD(T)] method together with the correlation-consistent polarized valence triple-zeta basis set, including diffuse functions (aug-cc-pVTZ).[34] These calculations are preliminary; they

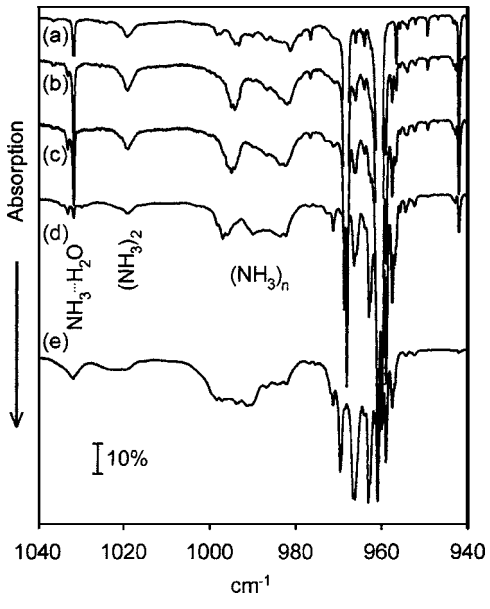

FIG. 4. Spectral regions of NH_3 ν_2 vibrational fundamental and $(NH_3)_n$ absorptions observed for Ne:NH_3:H_2=800:1:*x* deposits. (a)–(e) See Figs. 1(a)–1(e).

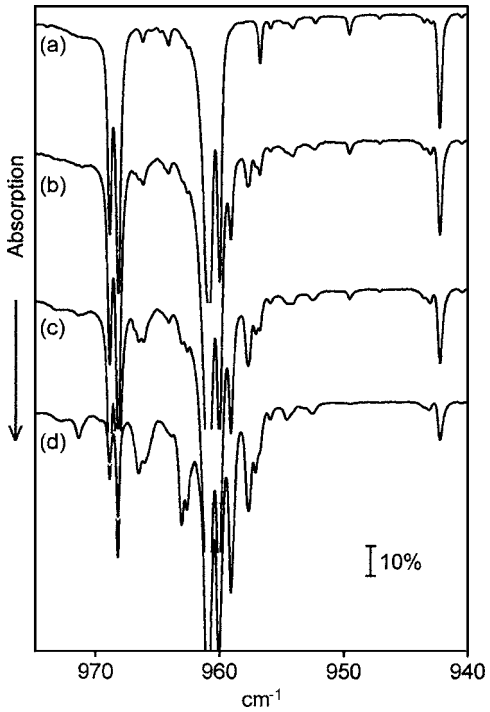

FIG. 5. Spectral region of NH_3 ν_2 vibrational fundamental observed for Ne:NH_3:H_2=800:1:*x* deposits. (a)–(d) See Figs. 1(a)–1(d).

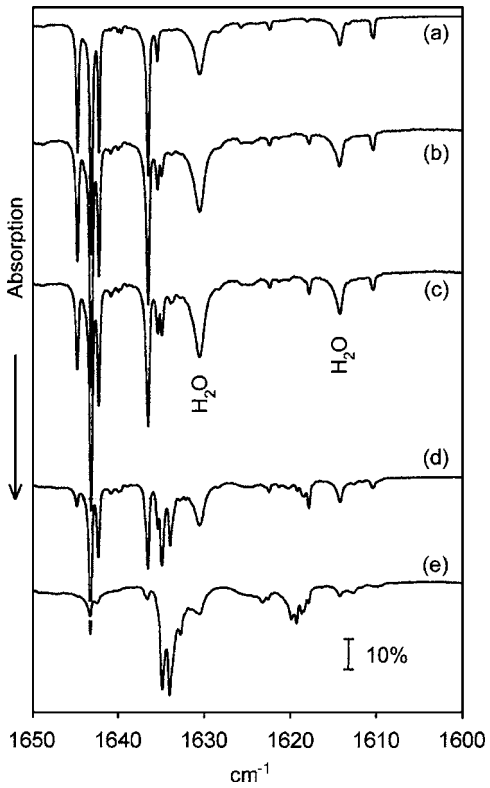

FIG. 6. Spectral region of NH_3 ν_4 vibrational fundamental observed for $Ne:NH_3:H_2=800:1:x$ deposits. (a)–(e) See Figs. 1(a)–1(e).

are not designed to treat large amplitude motions such as those of the NH_3 inversion and the low frequency motions of the weakly bound H_2 moiety.

A potential minimum was found for the axial complex, in which the H_2 serves as the proton donor and coordinates with the lone-pair electrons on the N atom of NH_3 to give a structure in which the H_2 is collinear with the threefold axis of the NH_3. The structure of this complex, illustrated in the upper part of Fig. 8, is summarized in Table III, which includes the structural parameters obtained in similar calculations for the NH_3 and H_2 moieties. The calculated N···H separation for the axial complex, 2.89 Å, compares closely with that recently calculated by Fawzy *et al.*[16] for the HH···NH complex, 2.85 Å. None of the distances between pairs of atoms in the NH_3 moiety was calculated to change by more than 0.001 Å from the corresponding distance for bonded and unbonded atom pairs obtained for uncomplexed NH_3.

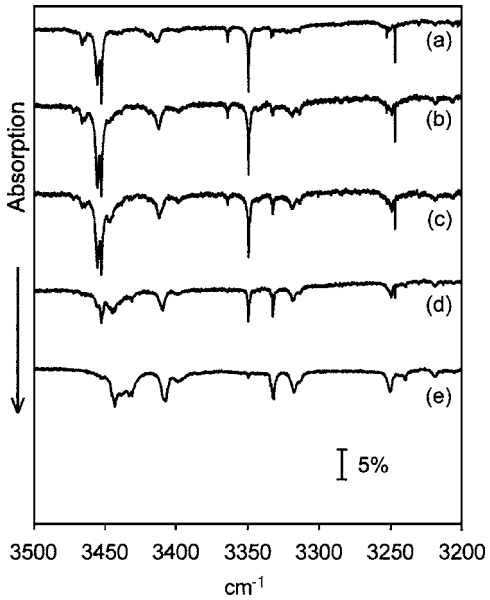

FIG. 7. Spectral regions of NH_3 ν_1 and ν_3 vibrational fundamentals and of NH_3 $2\nu_4$ observed for $Ne:NH_3:H_2=800:1:x$ deposits. (a)–(e) See Figs. 1(a)–1(e).

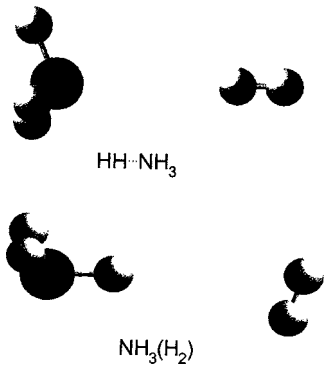

FIG. 8. Isomers of the van der Waals complex of H_2 with NH_3.

The potential minimum for the complex is 215 cm^{-1} (2.57 kJ/mol) lower in energy than the energy obtained in a BSSE-corrected single-point calculation for a structure which has a N···H separation increased by 10 Å, to 12.89 Å. From the single-point CCSD(T)/aug-cc-pVTZ calculations for the same pair of structures, the complex is 237 cm^{-1} (2.83 kJ/mol) lower in energy than the structure with the large N···H separation.

The harmonic vibrational fundamental frequencies obtained for NH_3, H_2, and the H_2···NH_3 complex are compared in Table IV. Complexation with H_2 is calculated to increase the harmonic frequency of the "umbrella" deformation (ν_2) of the NH_3 moiety by 9.3 cm^{-1}, but changes the position of each of the other three fundamentals by less than 5 cm^{-1}. When D_2 is substituted for H_2 in the axial complex, the positions of the vibrations contributed by the NH_3 moiety are unchanged from those for H_2···NH_3.

The estimated infrared intensity of the HH-stretching vibration obtained in the MP2 calculation is slightly greater than the sum of the intensities for the degenerate components of the NH_3 ν_3 vibration in the binary complex. Because the weak HD-stretching absorption of NH_3(HD) must arise from the complex with HD ($j=0$), it is probable that the coaxial structure is appropriate for the complex involving H_2 ($j=1$).

TABLE III. Calculated [RMP2/6-311++G(3*df*,3*pd*)] structures of the axial HH···NH_3 complex and of the molecules from which it is formed.

Coordinate	NH_3, H_2	HH···NH_3
R(N···H)		2.894 Å
R(N–H)	1.012 Å	1.012 Å
∠HNH	106.8°	106.7°
∠HN···H		111.9°
R(H–H)	0.737 Å	0.739 Å

TABLE IV. Calculated [RMP2/6-311++G(3*df*,3*pd*)] harmonic vibrational fundamentals (cm^{-1}) and infrared absorption intensities (km/mol, in parentheses) of the axial complexes of NH_3 with H_2 and D_2 and of the molecules from which it is formed. (Structure was not constrained to exact threefold symmetry. Values for both components of doubly degenerate vibrations are given.)

Vibration	NH_3, H_2, D_2	$HH\cdots NH_3$	$DD\cdots NH_3$
H_2 ω_{HH}	4516.8 0.00)	4480.1 (19)	
D_2 ω_{DD}	3195.1 (0.00)		3169.1 (10)
NH_3 ω_1 (a_1)	3519.1 (3)	3516.1 (2)	3516.1 (2)
NH_3 ω_2 (a_1)	1029.2 (147)	1038.5 (147)	1038.5 (147)
NH_3 ω_3 (e)	3667.8 (9)	3662.9 (9)	3662.9 (9)
	3665.6 (9)	3662.8 (9)	3662.8 (9)
NH_3 ω_4 (e)	1660.3 (14)	1661.0 (15)	1661.0 (15)
	1659.3 (14)	1661.0 (15)	1661.0 (15)
Complex deformation (e)		327.8 (1.6)	235.6 (3)
		327.7 (1.6)	235.4 (3)
$HH\cdots N$ stretch (a_1)		118.0 (0.6)	87.8 (0.4)
Complex deformation (e)		57.2 (48)	55.4 (49)
		56.8 (48)	55.0 (49)

Moreover, because the absorptions of isolated NH_3 diminish more readily upon adding H_2 or D_2 to the sample than upon adding HD, the axial complex is expected to be the more stable one.

In the search for another, less stable complex structure, optimizations at the RMP2/6−311++G(3*df*,3*pd*) level were attempted starting with the initial structure shown in the lower part of Fig. 8, similar to that for the $H_2\cdots HF$ complex[9] and for the H_2 ($j=0$) complex with H_2O.[12] In this structure, the center of mass of the H_2 is collinear with one of the NH bonds and the axis of the H_2 is oriented perpendicular to that NH bond and directed toward the NH_3 axis. A potential minimum was not found, but as the optimization proceeded the structure approached that for the axial complex. However, because the experiments have shown that a second H_2 molecule readily forms a complex with the initially formed $H_2\cdots NH_3$ and because NH_3 has only a single set of lone-pair electrons on the N atom, it is probable that a shallow potential minimum does exist for H_2 complexed with the H atom of the NH bond. Okumura *et al.*[35] studied the vibrational predissociation spectroscopy of the isoelectronic $(H_2)H_3O^+$ complex in the gas phase. Their observations were consistent with complexation at one of the H atoms. The addition of a second and third H_2 molecule to the complex occurs readily, and a total of three HH-stretching fundamentals—all close to 4046 cm^{-1}—resulted. Ion-molecule interactions are typically stronger than van der Waals interactions, consistent with this relatively large frequency shift in the HH-stretching absorptions.

The extent of rotation and inversion which the H_2 and NH_3 moieties can undergo in their binary complex(es) is of considerable interest. The results of the RMP2/6−311++G(3*df*,3*pd*) calculations for the axial $HH\cdots NH_3$ complex ignore the occurrence of large amplitude motions, predicting the harmonic vibrational energy levels of a rigid rotor. The three rotational constants given by the calculations for this complex, 190.247, 23.013, and 23.013 GHz (6.346, 0.768, and 0.768 cm^{-1}), indicate that it is a prolate symmetric top.

TABLE V. Calculated low-lying rotational energy levels $F(J,K)$ (cm^{-1}) of NH_3 and of its axial complexes with H_2 and D_2 for the rigid rotor approximation. [$F(J,K)=BJ(J+1)+(A-B)K^2$. The rotational constants, A and B, are obtained from the RMP2/6-311++G(3*df*,3*pd*) calculations for the appropriate species.]

$F(J,K)$	NH_3	$HH\cdots NH_3$	$DD\cdots NH_3$
$F(1,0)$	19.974	1.536	0.878
$F(1,1)$	16.327	7.114	6.785
$F(2,0)$	59.922	4.608	2.634
$F(2,1)$	56.275	10.186	8.541
$F(2,2)$	41.687	26.920	26.262
$F(3,0)$		9.216	5.268
$F(3,1)$		14.794	11.175

The calculated rotational constants for the axial complex of D_2 with NH_3 are 190.247, 13.168, and 13.168 GHz (6.346, 0.439, and 0.439 cm^{-1}). In contrast, the constants obtained in a similar calculation for NH_3 were 190.1, 299.6, and 299.2 GHz (6.340, 9.994, and 9.980 cm^{-1}), close to values appropriate for an oblate symmetric top. (We did not constrain the NH_3 to its known threefold symmetric structure.) Thus, very different rotational structures are anticipated for the spectra of NH_3 and $HH\cdots NH_3$. The positions $F(J,K)$ of the low-lying rotational energy levels of rigid NH_3 and $HH\cdots NH_3$ obtained from the MP2 calculations by using the familiar symmetric top relationship

$$F(J,K) = BJ(J+1) + (A-B)K^2,$$

where A and B are the rotational constants derived from the axial and nonaxial moments of inertia of the molecule and J and K are the rotational quantum numbers, are summarized in Table V. For a molecule trapped at 4.3 K, the Boltzmann factor governing the population of an energy level at 7.0 cm^{-1} is only 0.096 as large as that for the $J=0$ level.

There are two limiting cases for the vibrotational structure of the axial $HH\cdots NH_3$ complex. In the first of these cases, the complex rotates as a rigid unit, and the positions of the low-lying rotational energy levels are expected to be close to the calculated positions summarized in the third column of Table V. The relative positions of the low-J transitions for the vibrations of the rigid rotor complex are readily calculated from these energy levels. In the second limiting case, rigid NH_3 and H_2 moieties rotate independently of each other. Weida and Nesbitt[13] provided a detailed spectroscopic analysis for several bands of axial $H_2O\cdots HH$, which is isoelectronic with $HH\cdots NH_3$. They concluded that this pseudodiatomic model with slightly hindered rotation of the H_2 and H_2O moieties gives the most satisfactory description of that system. Application of this model to $HH\cdots NH_3$ would give a rotational structure in the vibrational bands of the complex which, if the inversion of the NH_3 moiety is neglected, would be close to that derived from the energy levels summarized in the second column of Table V.

The two NH-stretching fundamentals and the ν_4 deformation fundamental of NH_3 show only small inversion splittings which are not resolved for uncomplexed NH_3 isolated in a neon matrix. All of the absorptions which appear in the NH-stretching region are weak, and several of them are con-

tributed by $(NH_3)_n$ species. Consideration of this spectral region does not provide information on the nature or extent of rotation of the complex. For ν_4, absorptions of the binary complex with H_2 $(j=1)$ lie at 1617.9 and 1635.0 cm^{-1}. The rigid complex model predicts that the lowest excited energy levels are those for which (J,K) are (1,0), (2,0), and (1,1), in the order of their increasing energy. The positions of the ${}^rR(n,0)$ lines relative to the band origin are 7.114, 8.650, and 10.186 cm^{-1} for $n=0$, 1, and 2, respectively. Of these lines that for ${}^rR(0,0)$ should predominate. Other transitions which can be created from this subset of energy levels are ${}^pP(1,1)$, at -7.114 cm^{-1}, and ${}^pQ(1,1)$, at -5.578 cm^{-1}. If the observed absorption at 1635.0 cm^{-1} is assigned to the ${}^rR(0,0)$ transition of the rigid complex, a second absorption may be detectable at a frequency which is lower by 12.692 or 14.228 cm^{-1}. The absorption at 1617.9 cm^{-1}, all or most of which is contributed by the axial complex, lies 17.1 cm^{-1} below the 1635.0 cm^{-1} band. For the independent rigid rotor model, the lowest energy excited energy level is $F(1,1)$, at 16.327 cm^{-1}. As is summarized in Table II, for NH_3 isolated in solid neon the ν_4 ${}^pQ(1,1)$ absorption is much weaker than the ν_4 ${}^pP(1,1)$ peak. Using the energy level data calculated for a rigid NH_3 molecule, summarized in the second column of Table V, gives a ${}^rR(0,0)-{}^pP(1,1)$ separation of 32.654 cm^{-1}. The observed separation between the two observed absorptions of the axial complex in the NH_3 ν_4 spectral region is intermediate between the values calculated for the two models, but is closer to that for the rigid complex than to that for the independent rigid rotors.

If D_2 is substituted for H_2 in the complex, the rotational energy levels for the rigid complex are decreased, as is summarized in the fourth column of Table V. The ${}^rR(0,0)$ transition is calculated to lie 6.785 cm^{-1} above the band origin, and the ${}^pP(1,1)$ and ${}^pQ(1,1)$ transitions lie 6.785 and 5.907 cm^{-1} below the band origin, respectively. Depending on the assignment of the lower frequency band, the separation between the two observed bands for the rigid complex should be 13.570 or 12.692 cm^{-1}. Since for the independent rigid rotor model the rotation of the NH_3 is uncoupled from that of the H_2 or D_2, the separation in that model should again be 32.654 cm^{-1}. The observed separation for the $D_2\cdots NH_3$ complex in the present neon-matrix study is 16.8 cm^{-1}. This value differs by only 0.3 cm^{-1} from that for the complex with H_2, but this small decrease provides some support for a relatively rigid complex.

The infrared spectrum associated with ν_2 of NH_3 provides information regarding both rotation and inversion of the molecule. The relevant constants derived from the infrared spectra of NH_3 in the gas phase,[36] trapped in helium clusters,[37] and in solid neon[20] and argon[19] are summarized in Table VI. Approximate values for the position of the ν_2 band center are given for all of the systems by the expression $\frac{1}{2}[sQ(1,1)+aQ(1,1)]$. The analysis by Spirko and Kraemer[38] and by Colwell *et al.*[39] would permit use of the observed $J=0$ band origins of NH_3 to determine the ν_2 band center, yielding a refined value of 950.28 cm^{-1} for the gas-phase molecule. Since the corresponding analysis is not feasible for the spectrum of NH_3 in inert-gas media, for consistency the approximate value is given for all of the band centers listed in Table VI. In Table 12 of our recent paper, concerned with the assignment of the infrared spectrum of NH_3 trapped in solid neon,[20] an incorrect value was cited for the inversion splitting of NH_3 in helium clusters. The correct value[37] is given in Table III.

TABLE VI. Characteristics of ν_2 of NH_3 in various media. All quantities expressed in cm^{-1}.

	Gas phase[a]	He cluster[b]	Ne (site I)[c]	Ne (site II)[c]	Ar matrix[d]
Band center[e]	949.82	967	959.2	953.3	967.5
Inversion splitting[f]	36.4	24.6	19.3	21.8	23.7
Rotational spacing	20.10	15±1		15.7	ca. 19

[a]Reference 36.
[b]Reference 37.
[c]Reference 20.
[d]Reference 19.
[e]$\frac{1}{2}[sQ(1,1)+aQ(1,1)]$.
[f]$sQ(1,1)-aQ(1,1)$.

The inversion splitting in the very prominent ν_2 fundamental of NH_3 results in the appearance of two series—antisymmetric and symmetric—of rovibrational transitions, displaced to either side of the mean position of the two NH_3 $J=0$ band origins by half the magnitude of the inversion splitting. As is indicated in Table VI, for NH_3 trapped in site II this mean lies at approximately 953.3 cm^{-1}, and for NH_3 trapped in site I at 959.2 cm^{-1}. From Table II, the only absorption in the NH_3 ν_2 spectral region which can be attributed to the complex with H_2 $(j=1)$ lies at 957.7 cm^{-1}. The higher frequency peaks of the complex with H_2 and all of the peaks of the axial complex with D_2 may have been obscured by the strong absorptions of uncomplexed NH_3 in this spectral region. If it is presumed that the 957.7 cm^{-1} absorption arises from the $R(0,0)$ transition of the rigid complex, which, by definition, cannot invert, subtraction of the rotational spacing $(2B)$ of 1.536 cm^{-1} that was calculated for the rigid axial $HH\cdots NH_3$ complex would yield a band center at 956.2 cm^{-1}, a reasonable value. The independent rigid rotor model also presumes that the NH_3 moiety does not invert. For that model, the band origin should lie 19.974 cm^{-1} below the $R(0,0)$ peak, at about 938 cm^{-1}, a value significantly lower than any of the band centers given in Table VI.

Whether the approximate rigid rotor behavior exhibited by this weakly bound axial complex trapped in the neon matrix is intrinsic to the complex or is a result of inhibition of rotational motion by the surrounding neon atoms can only be determined by gas-phase observations.

IV. CONCLUSIONS

Complex formation between H_2 and NH_3 occurs readily. H_2 $(j=1)$ coordinates with the lone-pair electrons on the NH_3 molecule to form a complex in which the axis of the H_2 molecule is collinear with the threefold axis of the NH_3. The HH-stretching fundamental of the H_2 moiety in this complex exhibits a relatively prominent infrared absorption. Preliminary analysis of the infrared absorption pattern for this axial complex suggests that in the neon matrix its behavior approaches that for a rigid rotor. The observation of absorptions

of the binary complex of NH_3 with HD requires NH_3 also to form a complex with H_2 ($j=0$), but data do not suffice for determining the structure or the extent of rotation or inversion of the NH_3 molecule in its complex with H_2 ($j=0$) trapped in solid neon. Complexes of NH_3 with two or more H_2 molecules also contribute to the observed spectra.

ACKNOWLEDGMENT

Helpful conversations with Dr. Michael C. Heaven, of the Department of Chemistry at Emory University, are gratefully acknowledged.

[1] G. A. Olah, D. J. Donovan, J. Shen, and G. Klopman, J. Am. Chem. Soc. **97**, 3559 (1975).
[2] G. Danby, D. R. Flower, E. Kochanski, L. Kurdi, P. Valiron, and G. H. F. Diercksen, J. Phys. B **19**, 2891 (1986); G. Danby, D. R. Flower, P. Valiron, E. Kochanski, L. Kurdi, and G. H. F. Diercksen, *ibid.* **20**, 1039 (1987).
[3] A. Offer and D. R. Flower, J. Phys. B **22**, L439 (1989).
[4] A. Offer and D. R. Flower, J. Chem. Soc., Faraday Trans. **86**, 1659 (1990).
[5] G. Danby and P. Valiron, Chem. Phys. Lett. **163**, 75 (1989).
[6] D. E. Bernholdt, S. Liu, and C. E. Dykstra, J. Chem. Phys. **85**, 5120 (1986).
[7] C. M. Lovejoy, D. D. Nelson, Jr., and D. J. Nesbitt, J. Chem. Phys. **87**, 5621 (1987).
[8] K. W. Jucks and R. E. Miller, J. Chem. Phys. **87**, 5629 (1987).
[9] C. M. Lovejoy, D. D. Nelson, Jr., and D. J. Nesbitt, J. Chem. Phys. **89**, 7180 (1988).
[10] R. D. Hunt and L. Andrews, J. Chem. Phys. **86**, 3781 (1987).
[11] D. W. Schwenke, S. P. Walch, and P. R. Taylor, J. Chem. Phys. **94**, 2986 (1991); Q. Zhang, L. Chenyang, Y. Ma, F. Fish, M. M. Szczesniak, and V. Buch, *ibid.* **96**, 6039 (1992); T. R. Phillips, S. Maluendes, A. D. McLean, and S. Green, *ibid.* **101**, 5824 (1994); V. Balasubramanian, G. G. Balint-Kurti, and J. H. van Lenthe, J. Chem. Soc., Faraday Trans. **89**, 2239 (1993).
[12] V. Buch, J. Chem. Phys. **97**, 726 (1992).
[13] M. J. Weida and D. J. Nesbitt, J. Chem. Phys. **110**, 156 (1999).
[14] M. E. Fajardo, S. Tam, and M. E. DeRose, J. Mol. Struct. **695/696**, 111 (2004).
[15] D. Forney, M. E. Jacox, and W. E. Thompson, J. Chem. Phys. **121**, 5977 (2004).
[16] W. M. Fawzy, G. Kerenskaya, and M. C. Heaven, J. Chem. Phys. **122**, 144318 (2005).
[17] A. Moroz, R. L. Sweany, and S. L. Whittenburg, J. Phys. Chem. **94**, 1352 (1990).
[18] M. E. Jacox and W. E. Thompson, Phys. Chem. Chem. Phys. **7**, 768 (2005).
[19] L. Abouaf-Marguin, M. E. Jacox, and D. E. Milligan, J. Mol. Spectrosc. **67**, 34 (1977).
[20] M. E. Jacox and W. E. Thompson, J. Mol. Spectrosc. **228**, 414 (2004).
[21] Certain commercial instruments and materials are identified in this paper in order to specify adequately the experimental procedure. In no case does such identification imply recommendation or endorsement by the National Institute of Standards and Technology, nor does it imply that the instruments or materials identified are necessarily the best available for the purpose.
[22] M. E. Jacox and W. B. Olson, J. Chem. Phys. **86**, 3134 (1987).
[23] R. A. Toth, J. Opt. Soc. Am. B **8**, 2236 (1991); **10**, 2006 (1993).
[24] B. P. Stoicheff, Can. J. Phys. **35**, 730 (1957).
[25] H. P. Hopkins, Jr., R. F. Curl, Jr., and K. S. Pitzer, J. Chem. Phys. **48**, 2959 (1968).
[26] S. Süzer and L. Andrews, J. Chem. Phys. **87**, 5131 (1987).
[27] T. Nishiya, N. Hirota, H. Shinohara, and N. Nishi, J. Phys. Chem. **89**, 2260 (1985); A. J. Barnes, J. Mol. Struct. **237**, 19 (1990).
[28] H. Linnartz, W. L. Meerts, and M. Havenith, Chem. Phys. **193**, 327 (1995).
[29] M. Behrens, U. Buck, R. Fröchtenicht, M. Hartmann, and M. Havenith, J. Chem. Phys. **107**, 7179 (1997).
[30] A. Engdahl and B. Nelander, J. Chem. Phys. **91**, 6604 (1989).
[31] See EPAPS Document No. E-JCPSA6-124-004616 for Tables E1–E2 and Figs. E1–E6, concerned with the dependence of the positions and intensities of the infrared absorptions on the concentration of HD or of diatomic deuterium introduced into the sample mixture. This document can be reached via a direct link in the online article's HTML reference section or via the EPAPS homepage (http://www.aip.org/pubservs/epaps.html).
[32] M. J. Frisch, G. W. Trucks, H. B. Schlegel *et al.*, GAUSSIAN 03, Revision B.01, Gaussian, Inc., Wallingford, CT, 2004.
[33] S. F. Boys and F. Bernardi, Mol. Phys. **19**, 553 (1970); S. Simon, M. Duran, and J. J. Dannenberg, J. Chem. Phys. **105**, 11024 (1996).
[34] T. H. Dunning, J. Chem. Phys. **90**, 1007 (1989).
[35] M. Okumura, L. I. Yeh, J. D. Myers, and Y. T. Lee, J. Phys. Chem. **94**, 3416 (1990).
[36] R. L. Poynter and J. S. Margolis, Mol. Phys. **51**, 393 (1984).
[37] M. Behrens, U. Buck, R. Fröchtenicht, M. Hartmann, F. Huisken, and F. Rohmund, J. Chem. Phys. **109**, 5914 (1998).
[38] V. Spirko and W. P. Kraemer, J. Mol. Spectrosc. **133**, 331 (1989).
[39] S. M. Colwell, S. Carter, and N. C. Handy, Mol. Phys. **101**, 523 (2003).